1492–1500 *Nucleic Acids Research, 2006, Vol. 34, No. 5*
doi:10.1093/nar/gkj510

En masse nascent transcription analysis to elucidate regulatory transcription factors

Jinshui Fan, Ming Zhan[1], Jikui Shen[2], Jennifer L. Martindale, Xiaoling Yang, Tomoko Kawai and Myriam Gorospe*

Laboratory of Cellular and Molecular Biology and [1]Research Resources Branch, National Institute on Aging-Intramural Research Program, National Institutes of Health, Baltimore, MD 21224, USA and [2]Department of Ophthalmology, Johns Hopkins University School of Medicine, Baltimore, MD 21287, USA

Received December 22, 2005; Revised and Accepted January 30, 2006

ABSTRACT

Despite exhaustively informing about steady-state mRNA abundance, DNA microarrays have been used with limited success to identify regulatory transcription factors (TFs). The main limitation of this approach is that altered mRNA stability also strongly governs the patterns of expressed genes. Here, we used nuclear run-on assays and microarrays to systematically interrogate changes in nascent transcription in cells treated with the topoisomerase inhibitor camptothecin (CPT). Analysis of the promoters of coordinately transcribed genes after CPT treatment suggested the involvement of TFs c-Myb and Rfx1. The predicted CPT-dependent associations were subsequently confirmed by chromatin immunoprecipitation assays. Importantly, after RNAi-mediated knockdown of each TF, the CPT-elicited induction of c-Myb- and/or Rfx1-regulated mRNAs was diminished and the overall cellular response was impaired. The strategies described here permit the successful identification of the TFs responsible for implementing adaptive gene expression programs in response to cellular stimulation.

INTRODUCTION

In mammalian cells, damaging stimuli trigger the stress response, which is characterized by the coordinate expression of subsets of genes through both transcriptional and post-transcriptional mechanisms. Knowledge of stress-triggered transcriptional regulation has increased vastly in recent years through the elucidation of the signaling pathways, chromatin alterations and transcription factors (TFs) involved. Our understanding of the ensuing changes in expressed mRNAs has also expanded spectacularly through the utilization of the microarray technology. However, a systematic identification of the links between transcriptional regulatory events and the subsets of expressed transcripts has remained elusive due to two major obstacles. First, the combinatorial nature of TF function upon gene promoters. Since several TFs often bind to the promoters of eukaryotic genes in order to activate transcription, studying their individual and joint regulation is generally quite complex (1,2). Second, the strong contribution of altered mRNA stability in determining the patterns of expressed genes. Given that changes in mRNA half-life potently control the collections of expressed mRNAs, alterations in mRNA abundance may reflect changes in mRNA turnover rates instead of transcription (3–5).

Here, we focus on the analysis of newly transcribed (nascent) mRNAs in an effort to identify shared regulatory promoter elements and hence the TFs responsible for coordinating gene expression. Using HeLa cells treated with the topoisomerase I inhibitor camptothecin (CPT) as model system, the transcription of thousands of genes was assessed simultaneously using the nuclear run-on (NRO) assay and cDNA arrays. Comparison of the promoters present in the genes whose transcription was most robustly induced revealed highly conserved TF-binding sites, including those for c-Myb and Rfx1. This approach successfully identified TFs that were pivotal for the cell's response to genotoxic stress, as supported by additional studies demonstrating (i) the CPT-dependent association of c-Myb and Rfx1 with the promoters of predicted target genes, (ii) the requirement of c-Myb and Rfx1 for their transcriptional activation and (iii) the critical influence of Rfx1 and c-Myb on cell proliferation and survival after CPT treatment.

*To whom correspondence should be addressed at Box 12, LCMB, NIA-IRP, NIH, 5600 Nathan Shock Drive, Baltimore, MD 21224, USA. Tel: +1 410 558 8443; Fax: +1 410 558 8386; Email: myriam-gorospe@nih.gov
Correspondence may also be addressed to Ming Zhan, RRB, NIA-IRP, NIH, 5600 Nathan Shock Drive, Baltimore, MD 21224, USA. Tel: +1 410 558 8373; Fax: +1 410 558 8674; Email: zhanmi@mail.nih.gov

MATERIALS AND METHODS

Cell culture, small interfering (siRNA) transfection, cell toxicity measurements

Human cervical carcinoma HeLa cells were cultured in DMEM (Gibco) supplemented with 5% fetal bovine serum. Cells were transfected twice sequentially using Oligofectamine™ and 200 nM siRNA (Qiagen), treated with CPT (500 nM) for the times indicated and collected for the analysis of RNA, DNA or protein. c-Myb siRNA, AAGAGGUGGAAUCUCCAACUG; Rfx-1 siRNA, AAGACCUUCUGGAGGUACAAC; Ctrl siRNA, AAUUCUCCGAACGUGUCACGU (targeting genes expressed in the fungus *Ustilago maydis* and the bacterium *Thermotoga maritima*).

Hoechst 33342 (1 μg/ml) was added directly to the cell culture medium and nuclei were visualized and scored 10 min later from >1000 cells; three independent experiments were performed. To monitor [^{3}H]thymidine incorporation, cells were seeded in duplicate 6-well cluster plates (in each experiment, one cluster was used to measure [^{3}H]thymidine incorporation, the other for counting cells and calculating DNA concentration), cultured for 20 h and pulsed with 2 μCi/ml [^{3}H]thymidine at 37°C for 1 h. On ice, cultures were washed once with ice-cold KRB buffer (118 mM NaCl, 25 mM $NaHCO_3$, 5 mM KCl, 1.28 mM $CaCl_2$, 1.18 mM $MgCl_2$ and 1.17 mM KH_2PO_4) and precipitated by the addition of 2 ml/well ice-cold KRB containing 5% trichloroacetic acid (TCA) for 30 min. Samples were rinsed twice with ice-cold KRB and, following the addition of 1 ml 0.5 M NaOH/0.5% SDS, lysates were collected into scintillation vials. [^{3}H]thymidine incorporation was calculated as c.p.m./10^6 cells (c.p.m./μg DNA yielded similar results).

Nuclear run-on array analysis

NRO RNA was prepared and analyzed as described elsewhere (3,5) with some modifications. Fifty million cells were lysed in a buffer containing 20 mM Tris–HCl (pH 7.5), 20 mM NaCl, 5 mM $MgCl_2$, 0.25% [v/v] NP-40; the pelleted nuclei were lifted in suspension buffer [20 mM Tris–HCl (pH 7.5), 20 mM NaCl, 5 mM $MgCl_2$], layered onto a sucrose cushion [20 mM Tris–HCl (pH 7.5), 20 mM NaCl, 5 mM $MgCl_2$ and 1 M sucrose], spun at 600 *g* (4°C, 30 min) and resuspended in storage buffer [50 mM Tris–HCl (pH 8.3), 5 mM $MgCl_2$, 0.1 mM EDTA (pH 8.0) and 45% [v/v] glycerol]. For the NRO reaction, thawed nuclei (200 μl aliquots) were mixed with 200 μl of 2× NRO reaction buffer [10 mM Tris–HCl (pH 8.0), 300 mM KCl, 5 mM $MgCl_2$, 5 mM DTT, 0.5 mM of each rATP, rUTP and rGTP, and 1.2% sarcosyl] plus 500 μCi of [(α^{33}P]UTP (3000 Ci/mmol, 10 mCi/ml) and incubated for 30 min at 30°C with shaking, after which they were digested with DNase I (RNase-free) for 30 min at 37°C and then with proteinase K (1 μg/μl) for 1 h at 37°C. Nascent RNA, purified by filtration using Sephadex G-50 columns (Pharmacia), typically yielded ~3×10^8 c.p.m. MGC arrays (Mammalian Genome Collection, [http://www.grc.nia.nih.gov/branches/rrb/dna/array.htm, containing 9600 genes (6385 unique) spotted as full-length cDNAs http://mgc.nci.nih.gov/], were prehybridized for 2 h in Invitrogen Micro-Hyb™ buffer containing 10 μg Cot DNA and 8 μg poly(A), then the nascent radiolabeled RNA was added and hybridized for 48 h at 55°C. Following washes (2× SSC/0.1% SDS, 2× SSC/0.1% SDS and 1× SSC/0.1% SDS at 55°C), signals on the array filters were detected using a PhosphorImager (Pharmacia) and analyzed using the ArrayPro software (MediaCybernetics, Silver Spring, MD).

For data analysis, the raw intensities were transformed to $\log_{10}$, then used for the calculation of *Z*-scores, as described elsewhere (6). Significant changes in gene expression were calculated in the form of *Z*-ratios and *Z*-test values (7). All of the gene expression changes were assessed through comparison with untreated cells (time 0). The significance thresholds used in this study were *Z*-ratio values of ±1.50 and *Z*-test value of $P < 0.01$.

Computational analysis of promoters

Proximal promoter sequences for the 58 genes upregulated transcriptionally were available from the Promoser database (8). From each gene, 1.2 kb promoter sequences (1.0 kb upstream and 0.2 kb downstream of the transcription start site) were studied. The potential binding sites of TFs in each promoter were detected by scanning against the Transfac Profesional database (version 9.2) using the software Match for TF-binding site identification (www.biobase.com). Since TF-binding sites are short in sequence and many are degenerate, random, false positive hits appear frequently. To avoid this problem, we employed a comparative genomics approach based on the notion that bona fide promoters/enhancers exhibit conserved core functional domains and locations. For all of the up-regulated human genes, the mouse homologous counterparts were retrieved from the homologene database of NCBI. In total, 58 mouse homologous genes were obtained and the corresponding proximal promoters searched for TF-binding sites. Using similarity criteria of 0.95 for the core and 0.85 for the matrix (both ranging from 0 to 1), the top 10% most frequent TFs were chosen from human and mouse gene lists and those common between the two species were selected for further analysis.

Chromatin immunoprecipitation (ChIP) assay and quantitative PCR (Q-PCR)

Crosslinking of cells (~5×10^6 per treatment group) was performed in 1% formaldehyde for 10 min at 25°C and was stopped by adding 0.125 M glycine. Cells were washed twice with ice-cold PBS, then with ice-cold buffer I (0.25% Triton X-100, 10 mM EDTA, 0.5 mM EGTA and 10 mM HEPES, pH 7.0) and buffer II (200 mM NaCl, 1 mM EDTA, 0.5 mM EGTA and 10 mM HEPES, pH 7.0) and were lifted in 300 μl Lysis buffer (1% SDS, 10 mM EDTA, 50 mM Tris, pH 8.0 and 1× Roche Protease Inhibitor Cocktail). DNA was sheared to ~500 bp average size fragments using a Fisher Scientific Sonic Dismembrator (FS 100 Model, 60% output, 5 pulses, 5 s each). After sonication, insoluble cell debris was removed by centrifugation (21 000 *g*, 4°C, 10 min) and supernatants transferred to fresh 1.5 ml tubes. After assessing DNA concentration, DNA was diluted to 2 U (A_{260} units)/ml using dilution buffer (0.01% SDS, 1% Triton X-100, 2 mM EDTA, 150 mM NaCl, 20 mM Tris–HCl, pH 8.0 and 1× Roche proteinase inhibitor cocktail). The diluted samples (500 μl) were precleared for 4 h at 4°C with agitation by adding 50 μl of pretreated Protein A/G–Sepharose mixture 50% slurry

(Amersham). Beads were gently pelleted and the supernatants collected; after setting aside 1/10 vol of precleared lysate as input DNA, the remainder was divided equally into two parts for specific-antibody IP and control IP reactions.

IP reactions were carried out for 12 h at 4°C using 5 μg of specific antibodies (all from Santa Cruz Biotechnology). For IP of c-Myb, a mixture of rabbit anti-human-c-Myb (sc-7874x/H-141) and mouse anti-human-c-Myb (sc-8412x/C-2) antibodies was used; for IP of Rfx1, a mixture of two goat anti-human-Rfx1 antibodies (sc-10650x/D-19 and sc-10652x/I-19) was used; specific control IgGs (from mouse, goat, rabbit) were also from Santa Cruz Biotech. Following incubation with primary antibodies, 50 μl of pretreated Protein A/G–Sepharose slurry, 10 μg of sheared salmon sperm DNA and 50 μg of BSA were added and incubated for an additional 1 h. Precipitates were washed for 10 min each with TSE I (low-salt buffer, containing 0.1% SDS, 1% Triton X-100, 2 mM EDTA, 20 mM Tris–HCl, pH 8.1 and 150 mM NaCl), TSE II (high-salt buffer, containing 0.1% SDS, 1% Triton X-100, 2 mM EDTA, 20 mM Tris–HCl, pH 8.1 and 500 mM NaCl) and buffer III (LiCl buffer, containing 0.25 M LiCl, 1% NP-40, 1% deoxycholate, 1 mM EDTA and 10 mM Tris–HCl, pH 8.1). Precipitates were washed twice with TE buffer and the DNA eluted by incubating beads in 300 μl elution buffer (1% SDS, 0.1 M $NaHCO_3$) at 25°C for 15 min; after centrifugation at 4500 *g* (1 min), the eluted DNA was transfered to fresh tubes. Formaldehyde crosslinking was reversed by addition of NaCl (0.3 M final concentration) and 20 μg RNase A (Sigma), then heating at 65°C for 6 h. To purify the DNA fragments, eluates were digested with 50 μg/ml proteinase K (50°C, 2 h), then extracted with phenol:chloroform:isoamyl alcohol (25:24:1) and precipitated for 16 h using glycogen (20 μg) as carrier. The resulting DNA, dissolved in 100 μl TE, was used for Q-PCR analysis.

For Q-PCR analysis, all of the fragments were first amplified by regular PCR, purified from agarose gels, serially diluted (10^8–10^0) and used in Q-PCRs to prepare standard curves from which target gene fragment numbers were calculated in both IP DNA and 'Input' DNA (for normalization). Q-PCRs were performed using SYBR® Green, the oligomers listed below and the MJ Research Chrom4 thermal Cycler System (MJ Research Inc., Waltham, MA). Quality-control tests for the Q-PCR products were routinely performed by monitoring melting curves and the amplification of single DNA bands (Supplementary Data).

Oligomers for Q-PCR analysis after ChIP (for detailed promoter sequence information see Supplementary Data) FANCG, (for both c-Myb and Rfx1 IP) CGGGTCTGCGAAGCTCTGGGCT (forward) and GGTGTGGCAGCGAGGAAGGGC (reverse), yielding a 258 bp fragment; PANX1, (for both c-Myb and Rfx1 IP) CAAGGCTCTGATTGGGATGGCAG and GCAAGCGACTCTTTCTGTGGATGG, yielding a 293 bp fragment; POLD2, (for c-Myb IP) CCAGCCCACCGACCCAGGAG and GGATTAGCGAGTTGCGGCGATG, yielding a 151 bp fragment; (for Rfx1) GAGCCACACCCTCGGTTTCCTG and CGTGTCGCCATCGCTACAAGTG, yielding a 275 bp fragment; TFIP11, (for c-Myb IP) GGAATCCGCTGAGCCACCTTGG and TACAGGAATCACAGTCTTGACCTTC, yielding a 178 bp fragment; VAMP3, (for Rfx1 IP) AGGGCATTCTGTAACTGTTTGTAACT and GATGTTACTCCAGGACTCTCACTGTT, yielding a 341 bp fragment.

Total RNA analysis

Total RNA was extracted using STAT-60 (Tel-Test B, Friendswood, TX). RNA was treated with DNase I (Roche) to remove any contaminating genomic DNA and cDNA was synthesized using reverse transcriptase and random hexamers (Invitrogen). Q-PCR was performed as explained for ChIP-Q-PCR, using the primer pairs listed below. The abundance of mRNA was normalized to 18S rRNA.

Oligomers for Q-PCR to assess mRNA levels (each pair listed as forward and reverse); the specific positions of the primers and the fragments amplified are listed in the Supplementary Data. FANCG, ATGCCAGAAAAGGAACCAAGGAAC and TTACATCCCTGCTCACAGTTGAAAG, yielding a 201 bp fragment; PANX1, CCATTCCGACAGAAGACAGATGTTC and CCAAGGTTTGTCAGGAGTAGCATTG, yielding a 221 bp fragment; POLD2, GGCTGTTAAGATGCTGGATGAGATC and GCTGCTGTATCGGAAAATGTCACTC, yielding a 250 bp fragment; TFIP11, CCAAATCTTTCATGGACTTCGGCAG and GCTTCTTCCTCTGAGTCAACCACAG, yielding a 235 bp fragment; VAMP3, CAAGTAGATGAGGTGGTGGACATAATG and GCAGTTTTGAGTTCCGCTGGTTC, yielding a 267 bp fragment; 18S, GCTCCAATAGCGTATATTAAAGTTGCT and CCTCAGTTCCGAAAACCAACAAAATAG, yielding a 276 bp fragment.

Western blot analysis

For the detection of c-Myb, Rfx1, cleaved PARP, GAPDH and β-tubulin, whole-cell lysates were prepared in RIPA buffer and 10 μg aliquots were size-fractionated by SDS–PAGE for western blot analysis. Primary antibodies recognized c-Myb (Upstate Biotechnology), Rfx1 (Santa Cruz Biotechnology), GAPDH (Abcam), cleaved PARP (Cell Signaling Technology) or β-tubulin (Santa Cruz Biotechnology). Following secondary antibody incubations, signals were detected by enhanced chemiluminescence.

RESULTS AND DISCUSSION

En masse identification of newly transcribed genes by NRO and cDNA arrays

We present an approach (Figure 1) to identify specific TFs mediating the transcriptional control of gene expression based on the systematic analysis of *de novo* (nascent) transcription. The assessment of newly synthesized mRNA (using NRO) was chosen in order to circumvent the problematic influence of mRNA turnover on the pools of expressed mRNAs, since NRO analysis would allow the direct identification of bona fide transcriptionally regulated genes. The subsequent comparison of the corresponding promoter regions of these genes would then be used to elucidate the putative TFs involved. To test the validity of this approach, HeLa (human cervical carcinoma) cells were treated with the topoisomerase I inhibitor CPT [reviewed in Ref. (9)], a drug that elicited rapid, robust and consistent changes in gene transcription. The ensuing

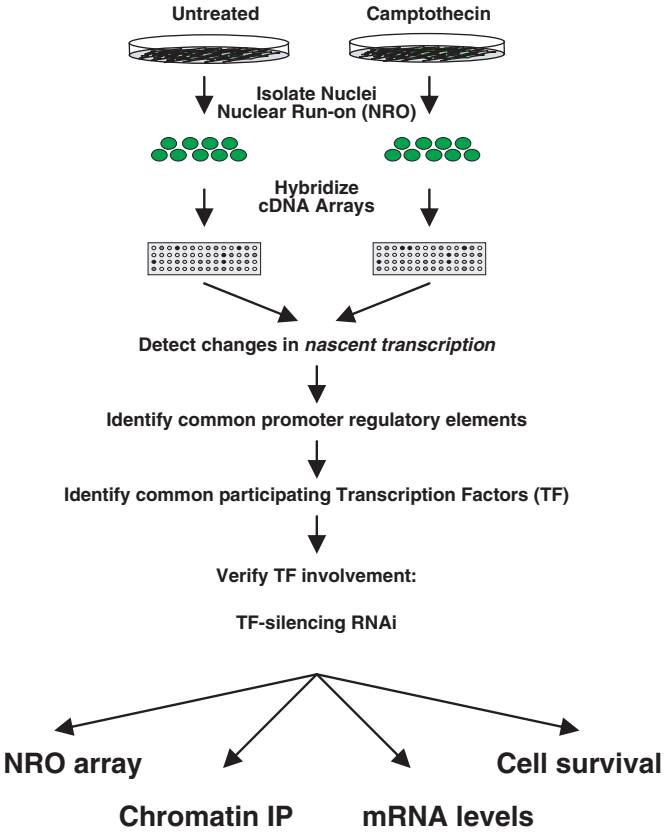

Figure 1. Schematic representation of the study. The goal of this investigation is to develop an approach that permits the identification of specific TFs governing the transcription of subsets of DNA damage-inducible genes. We sought to identify such regulatory TFs in HeLa cells following treatment with the topoisomerase I inhibitor CPT (500 nM, 2 h). Newly synthesized (nascent) mRNA was labeled by carrying out NRO reactions in the presence of [^{33}P]UTP and the relative levels of each nascent transcript in both untreated and CPT-treated populations were assessed by hybridization of cDNA arrays. A subset of genes was found to be transcriptionally upregulated using stringent statistical criteria and their promoters (1.0 kb upstream, 0.2 kb downstream of the transcriptional start site) were further studied by identifying the TF-binding sites present in them. TFs c-Myb and Rfx1 were found to be widely shared by almost all of the CPT-upregulated genes. To test the hypothesis that the identified TFs, c-Myb and Rfx1, were important regulators of gene expression following CPT treatment, their levels were silenced by RNAi. In the TF-knockdown cultures, the effect of c-Myb and Rfx1 on the response to CPT was investigated by the four additional analyses shown (i) performing NRO coupled with cDNA array analysis to monitor altered transcription rates of the putative target genes, (ii) carrying out ChIP to examine changes in the association of promoter DNA sequences with c-Myb and/or Rfx1, (iii) monitoring changes in total mRNA abundance, and (iv) assessing differences in the cellular response to CPT (specifically proliferation and survival).

transcriptional changes were systematically assessed by isolating nuclei from each cell population and carrying out NRO analysis, whereby individual RNA polymerase II molecules were allowed to resume on-going synthesis of endogenous transcripts in the presence of [α-^{33}P]UTP. The resulting radiolabeled nascent RNA products were then studied through hybridization of cDNA arrays, using methodologies described previously (3,6,7,10) and in Materials and Methods. For most genes, transcription remained unaltered following CPT treatment, as determined by monitoring NRO signals on the arrays, but a distinct subset of genes was transcriptionally upregulated and another subset was transcriptionally downregulated after

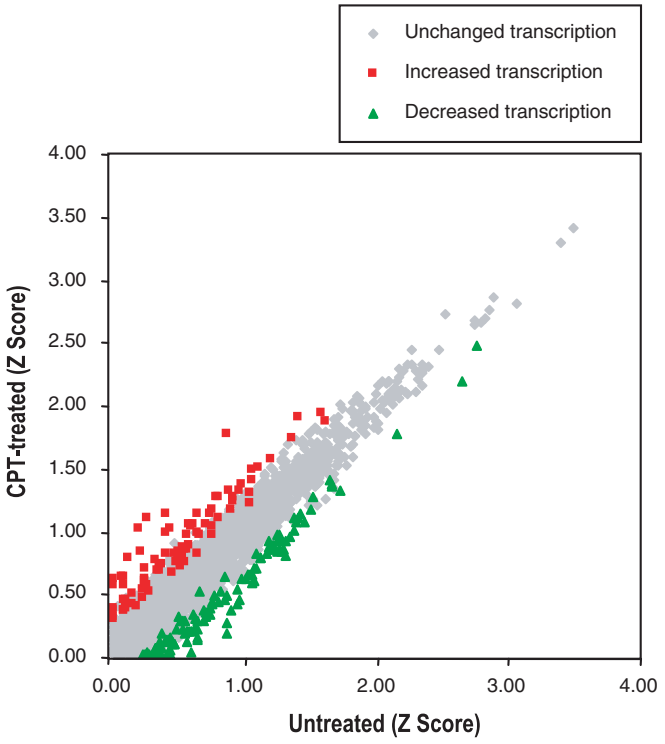

Figure 2. Transcriptional changes in untreated relative to CPT-treated populations. The relative transcriptional rates in untreated and CPT-treated populations, as assessed by monitoring signal intensities obtained from NRO arrays (*Z*-scores), were represented. Transcriptionally upregulated (red) and downregulated (green) RNA subsets are indicated.

CPT treatment (Figure 2). Control hybridizations conducted using samples from cells that had been treated with actinomycin D (an inhibitor of RNA polymerase II) indicated that the signals on the arrays were indeed derived from RNA polymerase II activity (Supplementary Data). Among the 85 genes that were transcriptionally upregulated, the proximal promoters (arbitrarily set at 1.0 kb upstream and 0.2 kb downstream of the transcription initiation site) were available for 58 genes and were thus chosen for further study.

Shared TF-binding sites in the promoters of transcriptionally upregulated genes

Table 1 lists the genes whose nascent transcription was upregulated by CPT; *Z*-ratio >1.5 [empirically found to correspond to >3-fold differences in signal intensity (data not shown)] and $P < 0.01$ values were chosen. There was some overlap between these genes and those identified as CPT-regulated in other high-throughput studies [including CDKN1A and DDB2 (11,12)], despite differences in cell lines employed, treatment conditions, array platforms and parameters measured (nascent RNA versus steady-state mRNA). The promoters corresponding to the genes in Table 1 were then analyzed using the PromoSer database (8). By considering similarity scores for TF-binding sites in these 58 promoters (with similarity values $\geq$0.95 and $\geq$0.85 for the core and matrix of each TF site, respectively), the presence (+) or absence (−) of binding sites on each promoter region for each TF were examined. Several TF sites that were either

Table 1. Genes transcriptionally upregulated by treatment with CPT

				Frequency of shared TF binding sites														
				High									Medium			Low		
Symbol	*Z*-ratio	*P*-value	RefSeq	c-Myb	Rfx1	AP-1	AREB6	Nkx2-5	Ik-1	Oct-1	Ets-1(p54)	Lmo2	NF-KB	c-Rel	USF	AHR	Pax-3	E2F
ABCF2	1.55	0.0001	NM_007189	+	+	+	+	+	+	+	+	+	−	+	−	−	−	−
AMPD2	1.75	0.0000	NM_004037	+	+	+	+	+	+	+	+	+	−	+	+	−	−	−
AP2M1	1.51	0.0006	NM_004068	+	+	+	+	+	+	+	+	+	−	−	−	−	−	−
APMCF1	2.17	0.0000	NM_021203	+	+	+	+	+	+	+	−	+	−	−	−	−	−	−
ASC	4.25	0.0000	NM_013258	−	+	+	+	−	+	+	+	+	+	−	−	−	−	−
BC-2	1.51	0.0008	NM_014453	+	+	+	+	+	+	+	+	+	−	+	−	−	−	−
CDCA4	1.72	0.0007	NM_017955	+	+	+	+	+	+	+	+	+	+	+	+	−	−	−
CDKN1A	4.68	0.0000	NM_078467	+	+	+	+	+	+	+	+	+	+	+	+	−	−	−
CDKN2D	1.58	0.0000	NM_001800	+	+	+	+	+	+	+	+	+	−	+	+	−	−	−
CHRNA3	1.59	0.0001	NM_000743	+	+	+	+	+	+	+	+	−	+	+	+	+	−	−
CIZ1	1.56	0.0012	NM_012127	+	+	+	+	+	+	+	+	+	+	+	+	−	−	−
CTXL	1.77	0.0032	NM_014312	−	+	+	+	+	+	+	+	+	+	+	−	−	−	−
DDX38	2.33	0.0000	NM_014003	+	+	+	+	+	+	+	+	+	−	−	−	−	−	−
DGCR8	1.73	0.0000	NM_022720	+	+	+	+	+	+	+	+	+	+	+	−	−	−	−
EGFR-RS	1.55	0.0000	NM_022450	+	+	+	+	+	+	+	+	+	+	+	−	−	−	−
EIF3S4	3.11	0.0000	NM_003755	+	+	+	+	+	+	+	+	+	−	−	+	−	−	−
FANCG	1.81	0.0001	NM_004629	+	+	+	+	+	+	+	+	+	−	+	−	−	−	−
FCER2	3.02	0.0000	NM_002002	+	+	+	+	+	+	+	+	+	−	+	+	−	−	−
GBA	1.77	0.0000	NM_000157	−	+	+	+	+	+	+	+	+	+	+	−	−	−	−
GEMIN4	2.01	0.0000	NM_015721	+	+	+	+	+	+	−	+	−	−	−	+	−	−	+
GPAA1	1.94	0.0045	NM_003801	−	−	+	+	+	+	+	+	+	+	+	+	−	−	−
GPCR1	2.55	0.0000	NM_014373	+	+	+	+	+	+	+	+	+	−	−	−	−	−	−
GPR30	1.54	0.0000	NM_001505	+	+	+	+	+	+	+	+	+	−	+	+	−	−	−
GRN	1.71	0.0000	NM_002087	+	+	+	+	+	+	−	+	+	+	−	+	−	−	−
HARS	1.60	0.0004	NM_002109	+	+	+	+	+	+	+	+	+	+	+	−	−	−	−
HSU79303	1.60	0.0001	NM_013301	+	+	+	+	+	+	+	+	−	+	+	−	−	−	−
HYAL3	1.66	0.0001	NM_003549	+	+	+	+	+	+	+	+	+	−	+	+	−	−	−
ISG20	2.45	0.0000	NM_002201	+	+	+	+	+	+	+	+	+	+	−	−	−	−	−
LOC51193	1.59	0.0000	NM_016331	+	+	+	+	−	+	−	+	+	+	+	+	−	+	−
MADH5	1.62	0.0000	NM_005903	+	+	+	+	+	+	+	+	+	+	−	+	−	−	−
MARS	1.52	0.0000	NM_004990	+	+	+	+	+	+	+	+	+	+	+	−	−	−	−
MATP	3.50	0.0000	NM_016180	+	+	+	+	+	+	+	+	−	+	−	+	−	−	−
MRPL10	1.77	0.0106	NM_148887	−	+	+	+	+	−	+	+	+	−	−	−	−	−	−
NCK1	2.33	0.0000	NM_006153	+	+	+	+	+	+	+	+	+	+	−	−	−	−	−
NEUGRIN	1.83	0.0000	NM_016645	−	+	+	+	+	+	+	+	+	−	−	+	−	−	−
NICN1	1.85	0.0000	NM_032316	+	+	+	+	+	+	+	+	+	−	+	+	−	−	−
NSPC1	2.00	0.0000	NM_032673	+	+	+	+	+	+	−	+	+	+	−	+	−	+	−
Nup37	1.65	0.0003	NM_024057	+	+	+	+	+	+	+	+	+	+	+	−	−	−	−
OGG1	1.83	0.0002	NM_016819	+	+	+	+	+	+	+	+	+	+	+	+	−	−	−
PANX1	1.93	0.0000	NM_015368	+	+	+	+	+	+	+	+	+	+	+	+	−	−	−
PB1	2.39	0.0000	NM_018165	−	+	+	+	+	+	+	+	+	−	+	−	−	−	−
POLD2	1.67	0.0009	NM_006230	+	+	+	+	+	+	+	+	+	+	+	+	−	−	−
POLG2	2.09	0.0000	NM_007215	+	+	+	+	+	+	+	+	−	−	+	+	−	−	−
PPP1CA	1.95	0.0001	NM_002708	+	+	+	+	+	+	+	+	+	+	+	+	−	−	−
PVR	2.94	0.0000	NM_006505	+	+	+	+	+	+	+	+	+	−	−	+	−	−	−
RNAHP	3.69	0.0000	NM_007372	+	+	+	+	+	+	+	+	+	+	+	+	−	−	−
RPS5	1.73	0.0000	NM_001009	+	+	+	+	+	+	+	+	+	−	+	+	−	−	−
RRM2	1.67	0.0004	NM_001034	+	+	+	+	+	+	+	+	+	+	+	+	−	−	+
SH3GLB2	1.59	0.0000	NM_020145	+	+	+	+	+	+	+	+	−	+	−	+	−	−	−
SNX5	1.67	0.0000	NM_152227	+	+	+	+	+	+	+	+	+	−	−	+	−	−	−
SRP	3.49	0.0000	NM_033199	+	+	+	+	+	+	+	+	+	−	−	+	−	−	−
STK16	1.55	0.0014	NM_003691	+	+	+	+	+	−	+	+	+	−	−	−	−	−	+
TAPBP-R	2.77	0.0000	NM_018009	−	+	+	+	+	+	+	+	+	+	+	+	−	−	−
TCEA2	1.68	0.0087	NM_003195	+	+	+	+	+	+	+	+	+	−	−	+	−	−	−
TFIP11	1.85	0.0048	NM_012143	+	+	+	+	+	+	+	+	+	−	−	−	−	−	−
TNFRSF7	3.96	0.0000	NM_001242	+	+	+	+	+	+	+	+	+	−	−	+	−	−	−
UQCR	1.51	0.0000	NM_006830	+	+	+	+	+	+	+	+	+	+	+	+	−	−	−
VAMP3	1.99	0.0000	NM_004781	+	+	+	+	+	+	+	+	+	−	−	−	−	−	−

Following treatment of HeLa cells with CPT for 2 h at 500 nM, nuclei were isolated for NRO analysis to detect nascent transcription using cDNA arrays (Materials and Methods). Promoter sequences were available for 58 transcriptionally upregulated genes (those genes showing *Z*-ratios >1.5 when comparing CPT-treated with untreated groups, and *P*-values <0.01); the analysis of these promoters revealed the presence of common binding sites for various TFs present at high, medium and low abundance. A TF-binding site was positive if the promoter sequence matched the consensus sequence with score values ⩾0.95 for the core and ⩾0.85 for the matrix of each TF. Plus, one or several TF-binding sites predicted; minus, no TF-binding sites predicted.

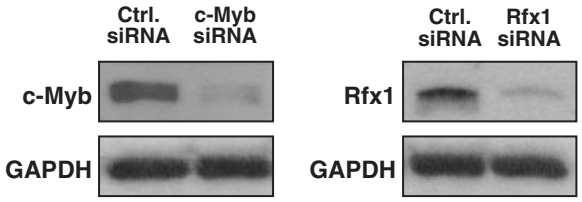

Figure 3. RNAi-mediated knockdown of c-Myb and Rfx1 in HeLa cells. Western blot analysis (20 μg protein per lane) to monitor the expression of c-Myb, Rfx1 and loading control GAPDH. HeLa cells (70% confluence) were transfected sequentially with Oligofectamine™ and siRNAs (200 nM) targeting either c-Myb or Rfx1 or with a control (Ctrl.) siRNA (Materials and Methods).

extensively shared (e.g. c-Myb through Lmo2), moderately shared (e.g. NF-κB, c-Rel, USF) or minimally shared (e.g. AHR, Pax-3, E2F) among the corresponding promoters are indicated. The potential binding sites of TFs in these promoters were also identified in the mouse orthologous genes (the complete lists for both species are available from the authors), showing extensive sharing of many TFs for these 58 genes, suggesting their evolutionary conservation and their possible co-regulatory function upon CPT-induced genes.

To test whether this approach could adequately identify shared regulatory TFs, we further assessed the influence of TFs Rfx1 and c-Myb [described in Refs (13–15)], for which binding sites were predicted on almost all of these promoters, on the expression of the predicted target genes. siRNA was employed to reduce the levels of Rfx1 or c-Myb to <15% of the levels seen in control (*Ctrl.*) populations (Figure 3); a simultaneous reduction of c-Myb and Rfx1 was not possible due to high toxicity seen after transfection to silence both TFs in the same cell (data not shown). NRO reactions and array analyses were then performed from each transfection group (untreated or treated with CPT for 2 h). Out of 58 genes 19 were found to be highly induced by CPT in the control siRNA transfection group, but were less induced in the c-Myb siRNA transfection group, the Rfx1 siRNA transfection group or both groups (Figure 4). Interestingly, in most of the genes examined, the binding sites of Rfx1 are adjacent to those of c-Myb (within 10 bp) and this distance was conserved in human and mouse homologous gene promoters, although the significance of this observations awaits further study. In addition to Rfx1 and c-Myb, binding sites of AREB6, AP-1, c-Ets-1(p54), Nkx2-5, Ik-1, Oct-1 and Lmo2 (Table 1) as well as Gfi-1, HNF-3beta, HFH-3, FOXJ2 and TGIF (data not shown) were highly frequent in both human and mouse gene lists. The transcription of the remaining two-thirds of the genes was unchanged despite the silencing of c-Myb or Rfx1, suggesting that their transcriptional increase after CPT treatment was regulated by other TFs. Taken together, these findings suggest that c-Myb, Rfx1 or both proteins were required for maximal transcriptional induction of a sizeable group of genes (19 out of 58) which had the corresponding TF-binding sites in their promoters (Table 1).

The identified TFs bind to the promoters of putative target genes and regulate mRNA abundance

Further verification of this regulatory scheme was undertaken by ChIP followed by real-time Q-PCR analysis to examine

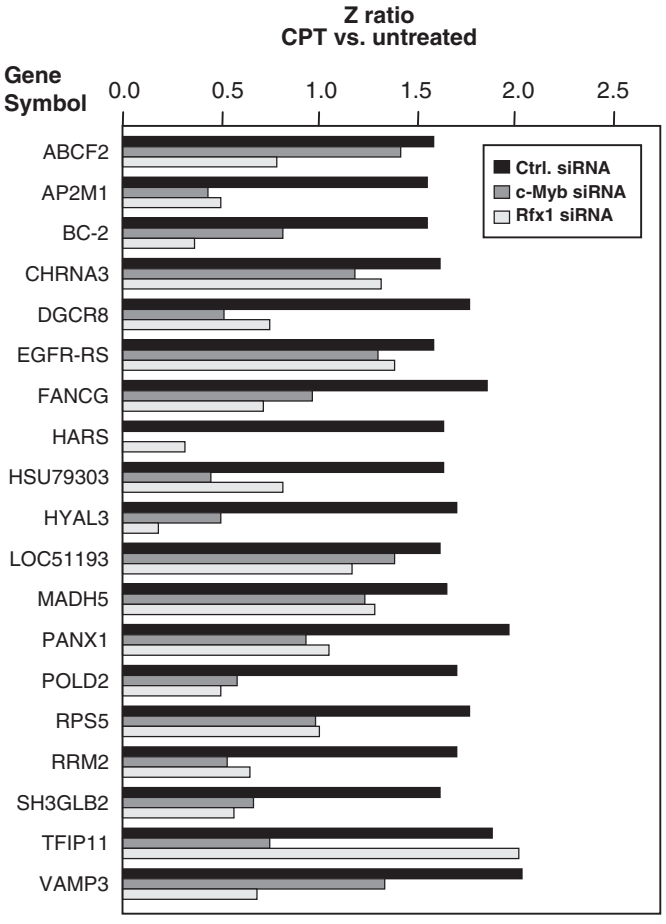

Figure 4. Impaired transcriptional upregulation of CPT-induced genes following c-Myb or Rfx1 knockdown. siRNA-transfected HeLa cells were either left untreated or treated with CPT (500 nM) for 2 h, whereupon nascent transcripts were prepared by NRO and assessed by array analysis (Materials and Methods). Shown are the *Z*-ratios of the nascent transcript signals (CPT-treated versus untreated) in each siRNA group. The genes on the graph have significant *Z*-ratios in the Ctrl. siRNA transfection group (≥1.5) and lower *Z*-ratios in either the c-Myb siRNA transfection group, the Rfx1 siRNA transfection group or both.

whether c-Myb, Rfx1 or both proteins physically associated with the promoters of target genes. Cells were crosslinked with formaldehyde to preserve the association of proteins with target DNA sequences, whereupon the DNA was sheared into ~500 bp fragments by sonication (Materials and Methods and Supplementary Data). Specific [TF–target DNA] complexes were subsequently immunoprecipitated using antibodies against c-Myb or Rfx1. Q-PCR was then employed to detect the presence of given promoter sequences in the ChIP material. As shown in Figure 5, the promoters of the predicted target genes FANCG, PANX1 and POLD2 were effectively immunoprecipitated in the control group, but not in populations with reduced c-Myb (*c-Myb siRNA*) or reduced Rfx1 (*Rfx1 siRNA*). Moreover, CPT induced the association of c-Myb and Rfx1 with the target gene promoters, but this interaction was unchanged or reduced in the c-Myb and Rfx1 siRNA groups. Similar observations were made when assessing the TFIP11 promoter, which was predicted to be primarily a target of c-Myb and with the VAMP3 promoter, which was predicted to preferentially associate with Rfx1 (Figures 4

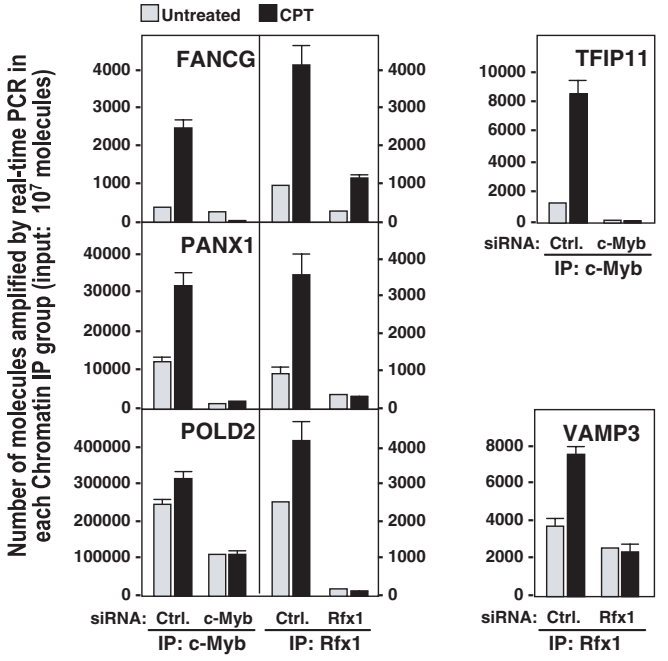

Figure 5. Quantitative ChIP analysis. ChIP analysis was performed essentially as described elsewhere (36). Following transfection (with Ctrl., c-Myb, Rfx1 siRNAs) cells were treated with CPT (2 h, 500 nM) and collected for analysis. Immunoprecipitations were carried out using anti-c-Myb, anti-Rfx1, or control IgG, whereupon Q-PCR was performed to amplify FANCG, PANX1, POLD2, TFIP11 or VAMP3 promoter regions (details in Materials and Methods). The absolute number of molecules amplified was calculated by carrying out parallel amplification curves with known substrate input quantities. Data are shown as the means from three independent biological triplicates and the SEMs.

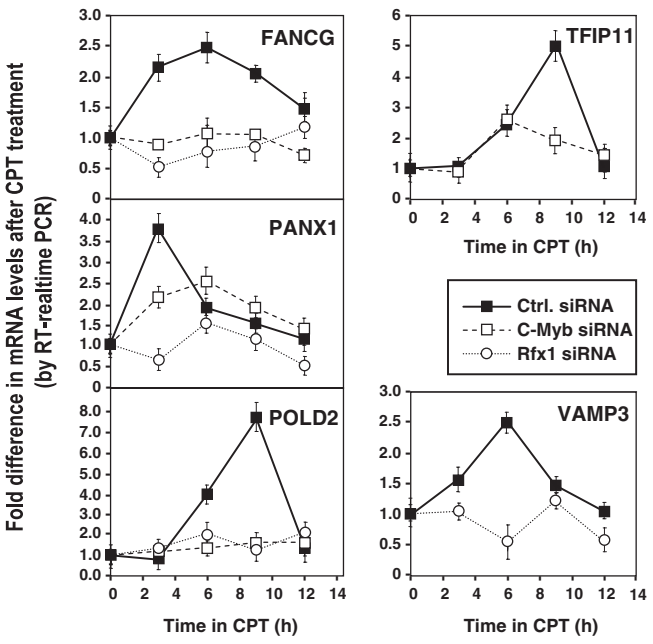

Figure 6. Quantitative mRNA analysis. Total RNA was extracted from the indicated siRNA groups at the times indicated following CPT treatment and mRNA levels calculated by Q-PCR using sequence-specific oligomer pairs and normalized to 18S rRNA levels (details in Materials and Methods). The absolute number of molecules amplified was calculated by carrying out parallel amplification curves with known substrate input quantities. Data are shown as the means and the SEM from three independent biological triplicates. Following c-Myb or Rfx1 silencing, the basal levels of these genes were either unchanged or modestly altered (up or down by 2-fold or less): FANCG mRNA was up by 2-fold (both siRNA interventions), PANX1 mRNA was slightly down and 2-fold up (after silencing c-Myb and Rfx1, respectively), POLD2 was unchanged and 2-fold down (after silencing c-Myb and Rfx1, respectively), TFIP11 mRNA was slightly down after silencing c-Myb, and VAMP3 was slightly elevated after silencing Rfx1.

and 5). An additional nine gene promoters were tested; among them, APG12L, ILF3, HSU79303 and NDUFB2 failed to show the expected enrichment in the c-Myb or Rfx1 IPs, while five did not yield any measurable promoter regions after Q-PCR, even after attempting to amplify multiple independent promoter segments for each gene. As anticipated, in control IgG IPs performed in parallel, no measurable promoter regions were amplified (data not shown).

Next, the influence of Rfx1 and c-Myb on the expression of the target genes was assessed directly by monitoring the steady-state levels of the corresponding mRNAs. In keeping with the notion that c-Myb and Rfx1 contributed to inducing target transcript levels following CPT treatment, Q-PCR analysis revealed that the levels of mRNAs encoding FANCG, PANX1, POLD2, TFIP11 and VAMP3 were elevated following CPT treatment, but this induction was attenuated or delayed if either c-Myb or Rfx1 were reduced (Figure 6). It is important to note that the assays used to obtain the results shown in Figures 4–6 measure different parameters (nascent transcription, association of a TF to a promoter region, accumulation of a given mRNA in the cell), so the magnitude of the changes could not be expected to match precisely; however, the trends are indeed consistent with one another on a qualitative level.

It is also important to recognize that the NRO methodology has significant limitations, including the facts that NRO data are semiquantitative and can have low sensitivity, specificity or both (whether derived from arrays or from traditional spotted nucleic acids). In addition, endogenous antisense transcripts can hybridize to the double-stranded cDNAs spotted on the arrays, while oligomer arrays might theoretically be used to circumvent this problem, it is technically impossible to achieve the sensitivity and specificity required with the tools presently available. These issues must be taken into consideration when interpreting NRO array data, since all of them have thus far been generated using cDNA arrays (3,5,16–18).

Taken together, these findings reveal that the analysis of nascent transcripts uniquely permits the identification of TFs which coordinate the expression of subsets of genes. Rfx1 and c-Myb, elucidated by this approach, were found to play critical roles in the cellular response to the genotoxic agent CPT. They were shown to associate with the promoters of the predicted target genes, binding was influenced by CPT treatment and knockdown of Rfx1 or c-Myb suppressed the CPT-induced expression of target genes. The varying degree of inhibition for the transcripts tested (Figure 4) likely depends on the influence of additional TFs independently acting upon the promoters and also on the possible effects of c-Myb and/or Rfx1-interacting proteins (19–21). It is important to note that c-Myb and Rfx1 have also been shown to operate as a transcriptional repressors (22,23). This regulatory function was not investigated here, although a number of genes were found to be upregulated in the Rfx1 siRNA treatment group (data not shown).

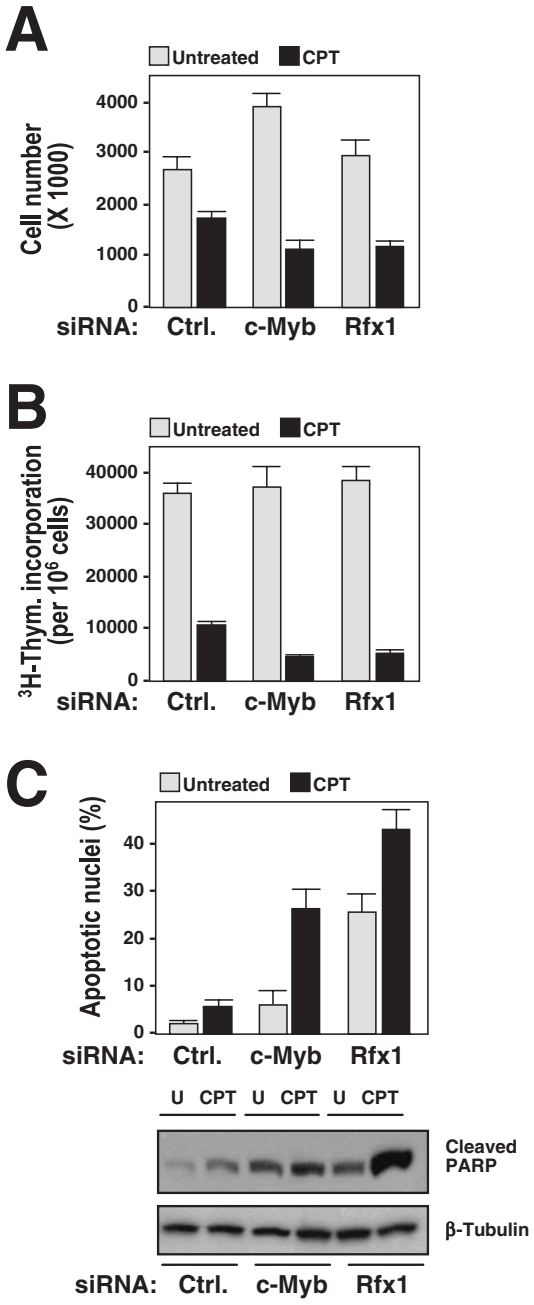

Figure 7. Influence of Rfx1 and c-Myb on the cellular response to CPT. (**A**) Forty-eight hours after each siRNA transfection, one million cells per transfection group were either left untreated or treated with CPT and the numbers of live cells were determined 24 h later by using a hemacytometer and trypan blue. (**B**) Cells that were transfected and treated with CPT as described in (A) were incubated for 1 h at 37°C with [^{3}H]thymidine (2 μCi/ml) and isotope incorporation was quantified. (**C**) Cells were transfected and treated with CPT as explained in (A) and 24 h later they were stained with Hoechst 33342 (1 μg/ml) for visualization and scoring of apoptotic (condensed or fragmented) nuclei. In (A–C), the data are shown as the means and SEMs from three independent biological triplicates.

Essential roles of c-Myb and Rfx1 in the cellular response to CPT

Finally, the influence of c-Myb and Rfx1 on the overall cellular response to CPT was evaluated by monitoring changes in cellular division, DNA replication and apoptosis of each population. As shown, c-Myb appeared to suppress proliferation slightly, since knocking down c-Myb resulted in increased cell numbers; however, silencing either c-Myb or Rfx1 significantly reduced cell numbers following CPT treatment (Figure 7A). Similarly, populations in which c-Myb or Rfx1 were knocked down incorporated significantly less [^{3}H]thymidine, suggesting that c-Myb and Rfx1 contributed to maintaining elevated levels of DNA replication in response to CPT treatment (Figure 7B). Moreover, apoptosis increased significantly after Rfx1 knockdown, even in cultures that were left without additional treatment (*U* populations) and was further elevated after CPT treatment in both c-Myb and Rfx1 siRNA groups, as monitored both by counting apoptotic (condensed or fragmented) nuclei and by assessing the levels of cleaved PARP (Figure 7C). Together, these findings suggest that Rfx1 and c-Myb exert a growth-regulatory, anti-apoptotic influence on HeLa cells exposed to CPT. The finding that c-Myb and Rfx1 are required for the optimal survival of CPT-treated HeLa cells is in keeping with the documented proto-oncogenic effects of c-Myb (24–27) and Rfx1 (28–31).

Perspectives

Most of our current understanding of the dynamics of expressed mRNA in mammalian systems comes from studies looking at steady-state mRNA abundance. However, a heightened interest in elucidating the TFs that regulate gene expression is driving the development of genome-wide methodologies to directly and systematically assess gene transcription and TF function. Indeed, the past few years have seen the development of powerful array-based and other high-throughput methods for ChIP and gene transcription analyses (16–18,32–35). The high-throughput, ChIP-derived strategies have the advantage of identifying all bound DNA at a genomic level, including previously unknown target regulatory regions, but have two significant limitations: they require prior knowledge of the involvement of a specific TF in a given response, and they provide little information on the functional consequences of the TF acting upon the particular genes (i.e. whether transcription is elevated, reduced or unaffected). The NRO array methodologies provide genome-wide information on transcriptional changes and do not require prior knowledge of the TFs involved, but fail to identify the factors that orchestrate the altered gene transcription programs. Here, we have reported a strategy which employs elements from both of these approaches. By obtaining *en masse* transcription data as a starting point, and coupling it to the analysis of the corresponding promoters, the TFs that drive transcriptional changes in response to a given stimulus can be systematically identified. We propose that the approaches described here can be widely applied to the identification of other TFs that orchestrate adaptive gene expression programs and shape the ensuing cellular responses.

ACKNOWLEDGEMENTS

We are grateful to our colleagues A. Jani, M. Fann, K. G. Becker, C. Cheadle and W. H. Wood,III for reagents, advice and assistance throughout this investigation. This work was supported in part by the Intramural Research Program of

the National Institute on Aging, National Institutes of Health. Funding to pay the Open Access publication charges for this article was provided by the National Institute on Aging-Intramural Research Program, NIH.

Conflict of interest statement. None declared.

REFERENCES

1. Chen,L. (1999) Combinatorial gene regulation by eukaryotic transcription factors. *Curr. Opin. Struct. Biol.*, **9**, 48–55.
2. Ogata,K., Sato,K. and Tahirov,T.H. (2003) Eukaryotic transcriptional regulatory complexes: cooperativity from near and afar. *Curr. Opin. Struct. Biol.*, **13**, 40–48.
3. Fan,J., Yang,X., Wang,W., Wood,W.H.,III, Becker,K.G. and Gorospe,M. (2002) Global analysis of stress-regulated mRNA turnover by using cDNA arrays. *Proc. Natl Acad. Sci. USA*, **99**, 10611–10616.
4. Khodursky,A.B. and Bernstein,J.A. (2003) Life after transcription—revisiting the fate of messenger RNA. *Trends Genet.*, **19**, 113–115.
5. Cheadle,C., Fan,J., Cho-Chung,Y.S., Werner,T., Ray,J., Do,L., Gorospe,M. and Becker,K.G. (2005) Control of gene expression during T cell activation: alternate regulation of mRNA transcription and mRNA stability. *BMC Genomics*, **6**, 75.
6. Cheadle,C., Vawter,M.P., Freed,W.J. and Becker,K.G. (2003) Analysis of microarray data using *Z* score transformation. *J. Mol. Diagn.*, **5**, 73–81.
7. Nadon,R., Woody,E., Shi,P., Rghei,N., Hubschle,H., Susko,E. and Ramm,P. (2002) Statistical inference in array genomics. In Geschwind,D. and Gregg,J. (eds), *Microarrays for the Neurosciences*. Cambridge, MIT Press.
8. Halees,A.S., Leyfer,D. and Weng,Z. (2003) PromoSer: a large-scale mammalian promoter and transcription start site identification service. *Nucleic. Acids. Res.*, **31**, 3554–3559.
9. Thomas,C.J., Rahier,N.J. and Hecht,S.M. (2004) Camptothecin: current perspectives. *Bioorg. Med. Chem.*, **12**, 1585–1604.
10. Kawai,T., Fan,J., Mazan-Mamczarz,K. and Gorospe,M. (2004) Global mRNA stabilization preferentially linked to translational repression during the endoplasmic reticulum stress response. *Mol. Cell. Biol.*, **24**, 6773–6787.
11. Zhou,Y., Gwadry,F.G., Reinhold,W.C., Miller,L.D., Smith,L.H., Scherf,U., Liu,E.T., Kohn,K.W., Pommier,Y. and Weinstein,J.N. (2002) Transcriptional regulation of mitotic genes by camptothecin-induced DNA damage: microarray analysis of dose- and time-dependent effects. *Cancer Res.*, **62**, 1688–1695.
12. Mariadason,J.M., Arango,D., Shi,Q., Wilson,A.J., Corner,G.A., Nicholas,C., Aranes,M.J., Lesser,M., Schwartz,E.L. and Augenlicht,L.H. (2003) Gene expression profiling-based prediction of response of colon carcinoma cells to 5-fluorouracil and camptothecin. *Cancer Res.*, **63**, 8791–8812.
13. Graf,T. (1992) A transcriptional activator linking proliferation and differentiation in hematopoietic cells. *Curr. Opin. Genet. Dev.*, **2**, 249–255.
14. Emery,P., Durand,B., Mach,B. and Reith,W. (1996) RFX proteins, a novel family of DNA binding proteins conserved in the eukaryotic kingdom. *Nucleic Acids Res.*, **24**, 803–807.
15. Oh,I.H. and Reddy,E.P. (1999) The myb gene family in cell growth, differentiation and apoptosis. *Oncogene*, **18**, 3017–3033.
16. Legen,L., Kemp,S., Krause,K., Profanter,B., Herrmann,R.G. and Maier,R.M. (2002) Comparative analysis of plastid transcription profiles of entire plastid chromosomes from tobacco attributed to wild-type and PEP-deficient transcription machineries. *Plant J.*, **31**, 171–188.
17. Schuhmacher,M., Kohlhuber,F., Holzel,M., Kaiser,C., Burtscher,H., Jarsch,M., Bornkamm,G.W., Laux,G., Polack,A., Weidle,U.H. *et al.* (2001) The transcriptional program of a human B cell line in response to Myc. *Nucleic Acids Res.*, **29**, 397–406.
18. Tenenbaum,S.A., Carson,C.C., Atasoy,U. and Keene,J.D. (2003) Genome-wide regulatory analysis using en masse nuclear run-ons and ribonomic profiling with autoimmune sera. *Gene*, **317**, 79–87.
19. Kaspar,P., Dvorakova,M., Kralova,J., Pajer,P., Kozmik,Z. and Dvorak,M. (1999) Myb-interacting protein, ATBF1, represses transcriptional activity of Myb oncoprotein. *J. Biol. Chem.*, **274**, 14422–14429.
20. Gajiwala,K.S., Chen,H., Cornille,F., Roques,B.P., Reith,W., Mach,B. and Burley,S.K. (2000) Structure of the winged-helix protein hRFX1 reveals a new mode of DNA binding. *Nature*, **403**, 916–921.
21. Korenjak,M., Taylor-Harding,B., Binne,U.K., Satterlee,J.S., Stevaux,O., Aasland,R., White-Cooper,H., Dyson,N. and Brehm,A. (2004) Native E2F/RBF complexes contain Myb-interacting proteins and repress transcription of developmentally controlled E2F target genes. *Cell*, **119**, 181–193.
22. Afroze,T. and Husain,M. (2000) c-Myb-binding sites mediate G(1)/S-associated repression of the plasma membrane Ca(2+)-ATPase-1 promoter. *J. Biol. Chem.*, **275**, 9062–9069.
23. Sengupta,P.K., Fargo,J. and Smith,B.D. (2002) The RFX family interacts at the collagen (COL1A2) start site and represses transcription. *J. Biol. Chem.*, **277**, 24926–24937.
24. Ganter,B. and Lipsick,J.S. (1999) Myb and oncogenesis. *Adv. Cancer Res.*, **76**, 21–60.
25. Gonda,T.J. (1998) The c-Myb oncoprotein. *Int. J. Biochem. Cell Biol.*, **30**, 547–551.
26. Introna,M. and Golay,J. (1999) How can oncogenic transcription factors cause cancer: a critical review of the myb story. *Leukemia*, **13**, 1301–1306.
27. Weston,K. (1999) Reassessing the role of C-MYB in tumorigenesis. *Oncogene*, **18**, 3034–3038.
28. Ostapchuk,P., Scheirle,G. and Hearing,G. (1989) Binding of nuclear factor EF-C to a functional domain of the hepatitis B virus enhancer region. *Mol. Cell. Biol.*, **9**, 2787–2797.
29. Siegrist,C.A., Durand,B., Emery,P., David,E., Hearing,P., Mach,B. and Reith,W. (1993) RFX1 is identical to enhancer factor C and functions as a transactivator of the hepatitis B virus enhancer. *Mol. Cell. Biol.*, **13**, 6375–6384.
30. Labrie,C., Lee,B.H. and Mathews,M.B. (1995) Transcription factors RFX1/EF-C and ATF-1 associate with the adenovirus E1A-responsive element of the human proliferating cell nuclear antigen promoter. *Nucleic Acids Res.*, **23**, 3732–3741.
31. Maijgren,S., Sur,I., Nilsson,M. and Toftgard,R. (2004) Involvement of RFX proteins in transcriptional activation from a Ras-responsive enhancer element. *Arch. Dermatol. Res.*, **295**, 482–489.
32. Sandoval,J., Rodriguez,J.L., Tur,G., Serviddio,G., Pereda,J., Boukaba,A., Sastre,J., Torres,L., Franco,L. and Lopez-Rodas,G. (2004) RNAPol-ChIP: a novel application of chromatin immunoprecipitation to the analysis of real-time gene transcription. *Nucleic Acids Res.*, **32**, e88.
33. Weinmann,A.S. (2004) Novel ChIP-based strategies to uncover transcription factor target genes in the immune system. *Nature Rev. Immunol.*, **4**, 381–386.
34. Impey,S., McCorkle,S.R., Cha-Molstad,H., Dwyer,J.M., Yochum,G.S., Boss,J.M., McWeeney,S., Dunn,J.J., Mandel,G. and Goodman,R.H. (2004) Defining the CREB regulon: a genome-wide analysis of transcription factor regulatory regions. *Cell*, **119**, 1041–1054.
35. Wells,J. and Farnham,P.J. (2002) Characterizing transcription factor binding sites using formaldehyde crosslinking and immunoprecipitation. *Methods*, **26**, 48–56.
36. Zhu,W., Giangrande,P.H. and Nevins,J.R. (2004) E2Fs link the control of G1/S and G2/M transcription. *EMBO J.*, **23**, 4615–4626.